Journal of Marine Research, 54, 631–651, 1996

Plankton production in tidal fronts: A model of Georges Bank in summer

by Peter J.S. Franks[1] and Changsheng Chen[2]

ABSTRACT

A two-dimensional (x,z) coupled physical-biological model of the plankton on Georges Bank during the summer was developed. The physical portion included a primitive-equation turbulence-closure model with topography-following σ coordinate. The biological model was a simple *N-P-Z* model. Tidal forcing at the model boundary generated a well-mixed region on the top of the bank, and strong tidal fronts at the bank edges. Biological fields were homogenized on the bank, while pronounced phytoplankton patches and horizontal gradients in properties developed in the fronts. The biomasses and fluxes of biological variables in the model agreed well with field estimates from Georges Bank. The phytoplankton in the well-mixed region of the bank were found to be nutrient replete, with f ratios of about 0.3. Values up to 0.7 were found for the f ratios in the fronts, where phytoplankton patches were supported by vertical fluxes of nutrients from below the euphotic zone. While the patterns of patchiness in the fronts were stable between tidal periods, the structure of patches and fluxes changed dramatically during a tidal cycle. Enhanced vertical mixing and horizontal gradients formed during a brief period of the tide, accounting for much of the cross-frontal nutrient flux. Sampling in such a dynamic system would be very difficult, and probably miss the essential features.

1. Introduction

Georges Bank is one of the most productive shelf ecosystems in the world (O'Reilly *et al.,* 1987; Cohen and Grosslein, 1987), having an annual area-weighted production two-to-three times that of the world's mean for continental shelves. Unlike many shelf ecosystems, the stratified summertime period makes an important contribution to the annual average primary production (O'Reilly *et al.,* 1987). Interdisciplinary field programs examining the physics and biology of the region have shown the high rates of production to be strongly linked to the unusual physical dynamics on the bank (e.g., Riley, 1941; Cohen *et al.,* 1982; Horne *et al.,* 1989), however the details of this linkage are poorly understood.

Strong tidal currents flowing over the abrupt bank topography create a well-mixed water column over the shallowest portion of the bank (e.g., Flagg, 1987). This well-mixed region

1. Scripps Institution of Oceanography University of California San Diego, La Jolla, California, 92093-0218, U.S.A.
2. Department of Marine Sciences, University of Georgia, Athens, Georgia, 30602-2206, U.S.A.

is separated from the stratified waters off the bank by dynamic tidal fronts. The strong horizontal temperature gradients at these fronts drive along-front jets, and cross-frontal residual currents (Garrett and Loder, 1981; Chen and Beardsley, 1995). The steep topography of the northern flank of the bank creates a more pronounced tidal front there than on the more gentle slope of the southern flank (Chen *et al.,* 1995). Field sampling has shown the dynamics of the northern tidal front to be very complicated, with the formation of transient hydraulic jumps, solitons propagating on and off-bank, breaking internal waves, and pronounced variations in mixing during a tidal cycle (Brickman and Loder, 1993; Loder *et al.,* 1992). All these processes can influence nutrient transports across the front and into the euphotic zone, and the formation of patches of swimming plankton (Franks, 1992a).

The hydrographic and dynamic properties of the tidal fronts surrounding the well-mixed central portion of the bank must influence the transports of nutrients onto the bank. It is not clear, however, to what degree the fronts enhance or hinder nutrient transport. Loder and Platt (1985) used scaling arguments to estimate the contributions of the fortnightly tidal excursion, baroclinic eddies, and frictionally induced currents to the cross-frontal transport of nutrients. They estimated that only about 9% of the nitrogen demand of phytoplankton on the bank could be met by these mechanisms. This would suggest an f ratio (ratio of production based on nutrients supplied from below the euphotic zone to total production) of about 0.1 on the bank, and imply that regenerative processes were dominant in supplying nutrients to the bank phytoplankton. On the other hand, using ^{15}N uptake techniques, Horne *et al.* (1989) found summertime f ratios of 0.23–0.3 on the bank, and values up to 0.7 in the frontal regions, indicating that one- to two-thirds of the nutrients used in phytoplankton production were "new" nutrients (cf. Dugdale and Goering, 1967; Eppley and Peterson, 1979), i.e., supplied by physical processes.

Recurrent patterns of plankton patchiness have been recorded on Georges Bank. The waters over the central bank are vertically well mixed, containing a region of unusually high chlorophyll (O'Reilly *et al.,* 1987; Sathyendranath *et al.,* 1991). Strong patches of high chlorophyll are often seen in the northern tidal front (Horne *et al.,* 1989; O'Reilly *et al.,* 1987), similar to the distribution of phytoplankton at other tidal fronts (e.g., Holligan, 1981; Pingree *et al.,* 1975). Strong horizontal gradients of nutrients, phytoplankton and zooplankton are associated with the tidal fronts at the bank's edges, however the detailed relationship of these patterns with the dynamic tidal fronts has not been elucidated.

To examine the physical and biological mechanisms controlling plankton production and patchiness on Georges Bank during the summer, we have developed a coupled primitive-equation/turbulence-closure/ecosystem model configured for a two-dimensional (x,z) section across Georges Bank. So far as we know, this model architecture is the first of its kind for use in oceanography in combining the primitive-equation and second-order turbulence closure physical models with an ecosystem model. The model was found to give excellent agreement with available biological and physical data, and gives us insight into the mechanisms supporting the primary production and patchiness on the bank.

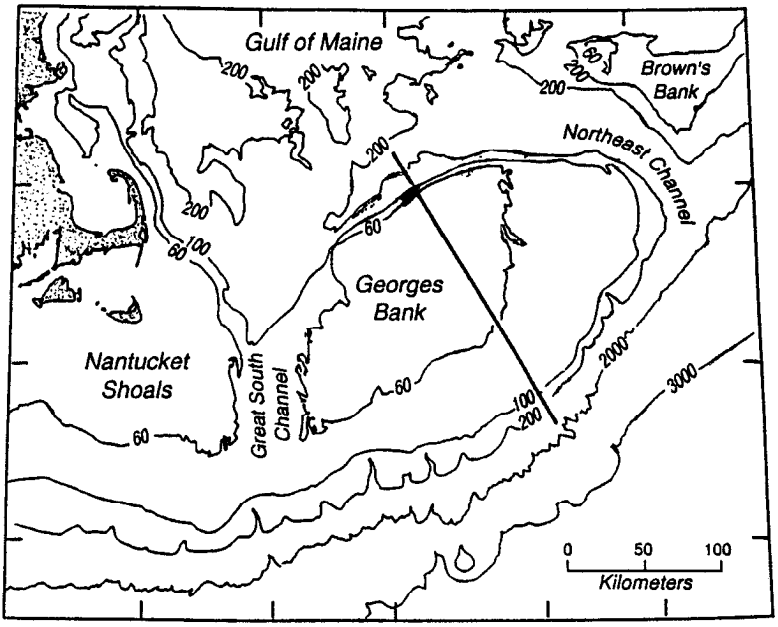

Figure 1. Bathymetry (in meters) of the southern Gulf of Maine and Georges Bank (Uchupi and Austin, 1987). The heavy line is the cross-bank section used in the numerical model.

2. Physical model

This study used the coastal ocean circulation model developed by Blumberg and Mellor (1987), modified to include the Mellor and Yamada (1982) level 2.5 turbulence-closure model. The turbulence-closure model provides a realistic parameterization of vertical mixing, and a free surface which allows the propagation of tides and other long surface gravity waves. The model also incorporates a semi-implicit scheme in the horizontal for the time stepping of the barotropic mode (Casulli, 1990), which improves the computational efficiency. A σ coordinate system is used in the vertical, and a non-uniform grid in the horizontal. Detailed descriptions of the model can be found in Blumberg (1994), Chen and Beardsley (1995) and Chen *et al.* (1995).

The two-dimensional model domain represents a cross-bank section from the northwest to the southeast, through the center of Georges Bank (Fig. 1). The bottom topography is taken from Uchupi and Austin (1987). The spacing of the nonuniform horizontal grid (Fig. 2) increases linearly from 1.0 km on and near the bank to 11.96 km off the bank outside the region of interest. The σ coordinate system in the vertical gives the same number of vertical grid points regardless of bottom depth. With 61 grid points, the vertical resolution thus varies from about 5 m off the bank (300 m depth) to <1 m over the shallow region of the bank (40 m depth).

The model is forced with an M_2 tide at the southern open boundary. To allow the propagation of tidal waves out of the computational domain with minimum reflection, a

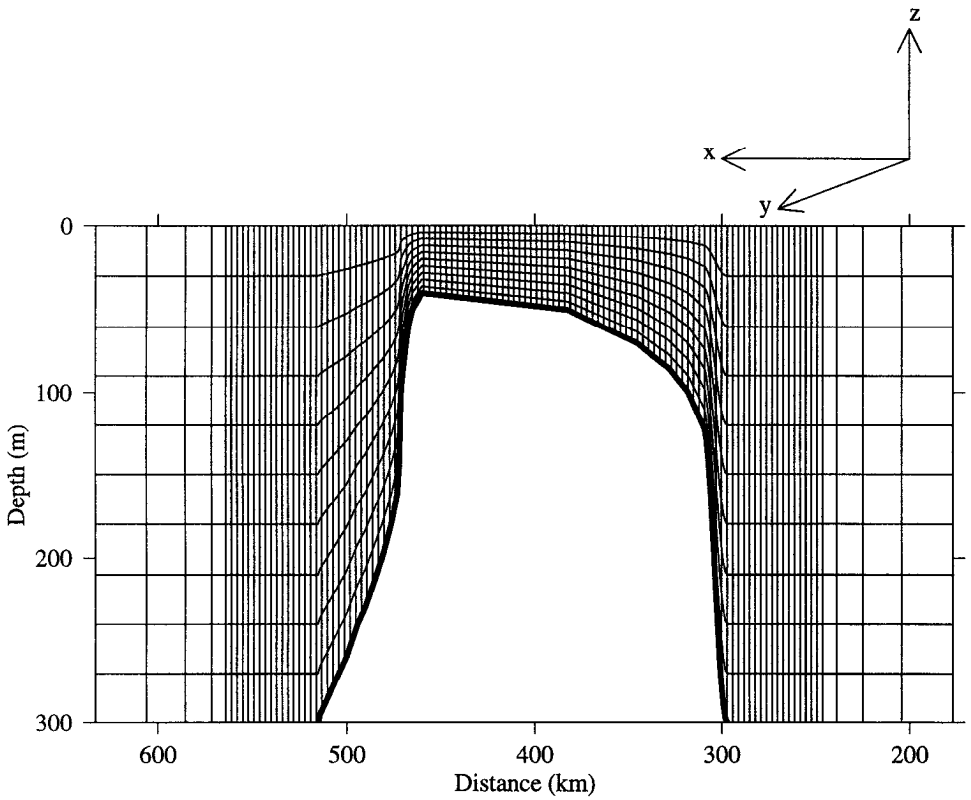

Figure 2. Numerical model grid, plotted every six points in the vertical and every three in the horizontal. Horizontal spacing is 1 km over the bank from 249 to 561 km, and then increases linearly to 11.96 km over 15 grid points away from the region of interest. The vertical grid spacing for σ is $\Delta\sigma = 0.0166$, where $0 \leq \sigma \leq 1$. Note that x increases to the left, toward the northwest.

sponge layer and a gravity wave radiation condition were specified at the northern open boundary. A free surface tidal amplitude of 90 cm produces a cross-bank barotropic surface tidal current of about 12 cm s^{-1} in the deep region, and about 90 cm s^{-1} over the bank, consistent with data from Moody *et al.* (1984).

The model was initialized with a linearly stratified temperature field, decreasing from 20°C at the surface, to 11°C at 300 m. Salinity was homogeneous at 35 psu. This strongly stratified field is representative of summertime conditions over the bank (e.g., Flagg, 1987). The tidal forcing was ramped up from zero to full amplitude over 1.5 days. Residual flows and mean fields were obtained by averaging over one complete tidal cycle.

3. Biological model

The biological model was the simple nutrient-phytoplankton-zooplankton (*NPZ*) model of Franks *et al.* (1986) (Fig. 3). Nitrogen is used as a tracer for the state variables.

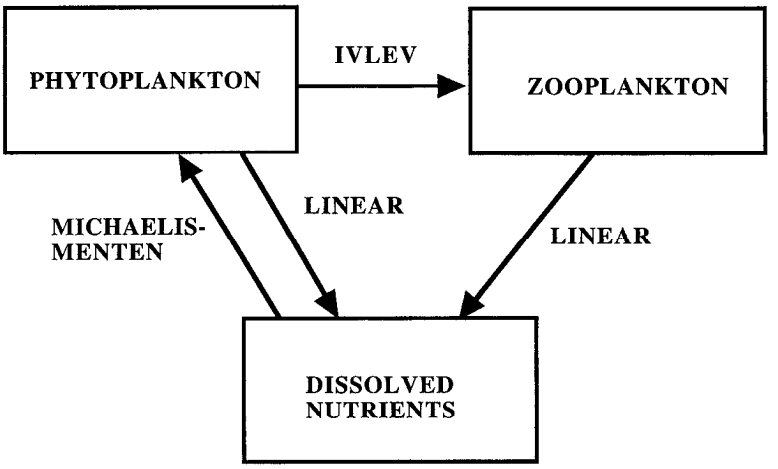

Figure 3. Schematic of the state variables and fluxes of the *N-P-Z* model of Franks *et al.* (1986).

Dissolved nutrients are taken up by the phytoplankton following Michaelis-Menten kinetics, while phytoplankton are grazed by zooplankton with an Ivlev functional response:

$$\frac{dP}{dt} = \frac{V_m N}{k_s + N} f(I_o)P - ZR_m(1 - e^{-\lambda P}) - \epsilon P \tag{1}$$

$$\frac{dZ}{dt} = \gamma ZR_m(1 - e^{-\lambda P}) - gZ \tag{2}$$

$$\frac{dN}{dt} = -\frac{V_m N}{k_s + N} f(I_o)P + (1 - \gamma)ZR_m(1 - e^{-\lambda P}) + \epsilon P + gZ, \tag{3}$$

where P is phytoplankton, Z zooplankton and N dissolved nutrient, all in μmole N l^{-1}. The total amount of nutrient, N_T, is conserved: $N + P + Z = N_T$.

There are seven parameters governing the Franks *et al.* (1986) model. The maximal phytoplankton nutrient uptake rate (and growth rate) is V_m, with a half-saturation constant k_s. The zooplankton have a maximal grazing rate R_m, with the grazing efficiency controlled by λ. Only a portion, γ, of the ingested phytoplankton is assimilated by the zooplankton, the remainder being recycled into dissolved nutrients. Both phytoplankton and zooplankton die at rates ϵ and g respectively. These dead fractions are immediately recycled into dissolved nutrients. The phytoplankton depend on incident irradiance I_o through the function $f(I_o)$ which we have taken to be linear:

$$f(I_o) = I_o e^{-k_{ext}z} \tag{4}$$

where k_{ext} is the diffuse attenuation coefficient for irradiance and z is depth below the surface. No dependence of k_{ext} on the local particle (phytoplankton) concentration was included.

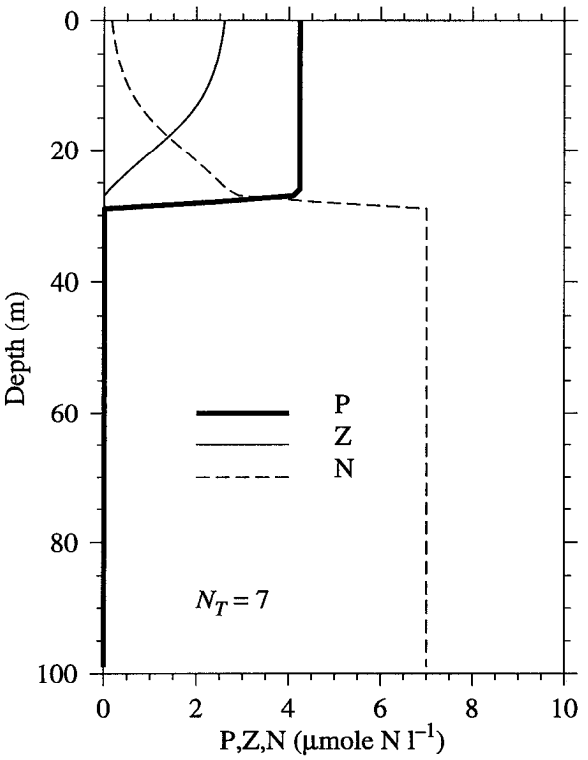

Figure 4. Initial condition for the biological variables. P, Z and N were initialized at steady state, with no horizontal dependence. The total nutrient, N_T = 7 μmole N l^{-1}. The diffuse attenuation coefficient was 0.1 m^{-1}. The phytoplankton growth rate decreases exponentially with irradiance, leading to a decreasing zooplankton biomass with depth. The decrease in zooplankton biomass is balanced by an increase in dissolved nutrients, while the phytoplankton biomass is constant throughout the euphotic zone.

The *NPZ* model of Franks *et al.* (1986) has an analytical steady-state solution which was used to initialize the coupled physical-biological model (Fig. 4). Thus during the model runs, any changes in the biological state variables must have been caused by physical forcings, allowing a clear separation of physical and biological dynamics in the formation of biological features. Since there is no dependence of any state variable on temperature, and no variation in k_{ext} across the bank, there is no horizontal dependence of the initial condition for the biological state variables. While these assumptions are not realistic, they are conservative in the sense that any horizontal patchiness which develops during the simulation must have arisen from physical-biological couplings rather than underlying horizontal gradients.

The parameter values were chosen based on a variety of sources (Table 1). The total amount of nutrient, N_T, was taken from the wintertime surface nitrate concentrations on Georges Bank of 7 μmole N l^{-1} (Pastuszak *et al.*, 1982). The phytoplankton uptake

Table 1. Parameter values for the biological model.

Parameter	Description	Value
V_m	maximum nutrient uptake rate	2 d^{-1}
k_s	half-saturation constant for nutrient uptake	1 μmole N l^{-1}
R_m	maximum grazing rate	0.5 d^{-1}
g	zooplankton death rate	0.2 d^{-1}
λ	Ivlev constant for grazing	0.2 (μmole N l^{-1})$^{-1}$
ϵ	death rate of phytoplankton	0.1 d^{-1}
γ	proportion of excreted nutrient by zooplankton	0.3
k_{ext}	diffuse attenuation coefficient	0.1 m^{-1}
N_T	total amount of nutrient	7 μmole N l^{-1}

parameters are typical of coastal diatoms (e.g., Eppley *et al.*, 1969; Falkowski, 1975), while the zooplankton grazing parameters fall in the range found for *Calanus finmarchicus, Psuedocalanus* sp. and *Centropages hamatus* (e.g., review in Fransz *et al.*, 1991), the dominant copepods on the bank during the summer (Davis, 1987). The diffuse attenuation coefficient was calculated from the 1% light depths reported in O'Reilly *et al.* (1987) for summer. Phytoplankton sinking speeds were set at 1 m day^{-1} (e.g., Bienfang, 1981; Granata, 1991).

4. Results and discussion

Model results and animations beyond those presented in this manuscript can be found on the world-wide web at the address *http://spiff.ucsd.edu/index.html.*

The coupled physical-biological model reached a steady periodic cycle by the 20th tidal cycle; there was little change in the tidal-average fields from cycle to cycle. The results presented below show both tidal-average fields, and details of the dynamics from the northern tidal front during the 25th tidal cycle.

a. Tidal-average fields

Physical. The behavior of the physical model is explored in detail in Chen and Beardsley (1995) and Chen *et al.* (1995), and is only briefly described here. The propagation of the M_2 tide over the bank topography generated a well-mixed region in the shallow waters over the bank, separated from the stratified waters off the bank by tidal mixing fronts (Fig. 5). The northern tidal front was located at about the 40 m isobath, while the front on the southern flank was between the 50 and 60 m isobaths. A slight horizontal gradient in temperature across the vertically well-mixed portion of the bank is consistent with observations in Loder *et al.* (1982). Tidally rectified flows in the fronts caused a strong along-front jet to the east on the northern flank of the bank (maximum 32 cm s^{-1}), and a broader, weaker jet to the west on the southern flank (maximum 8 cm s^{-1}), in good agreement with observations (Chen *et al.*, 1995).

Strong cross-frontal residual (i.e., tidal average) circulations are generated within the tidal fronts. On the southern flank multi-celled circulations developed, associated with the

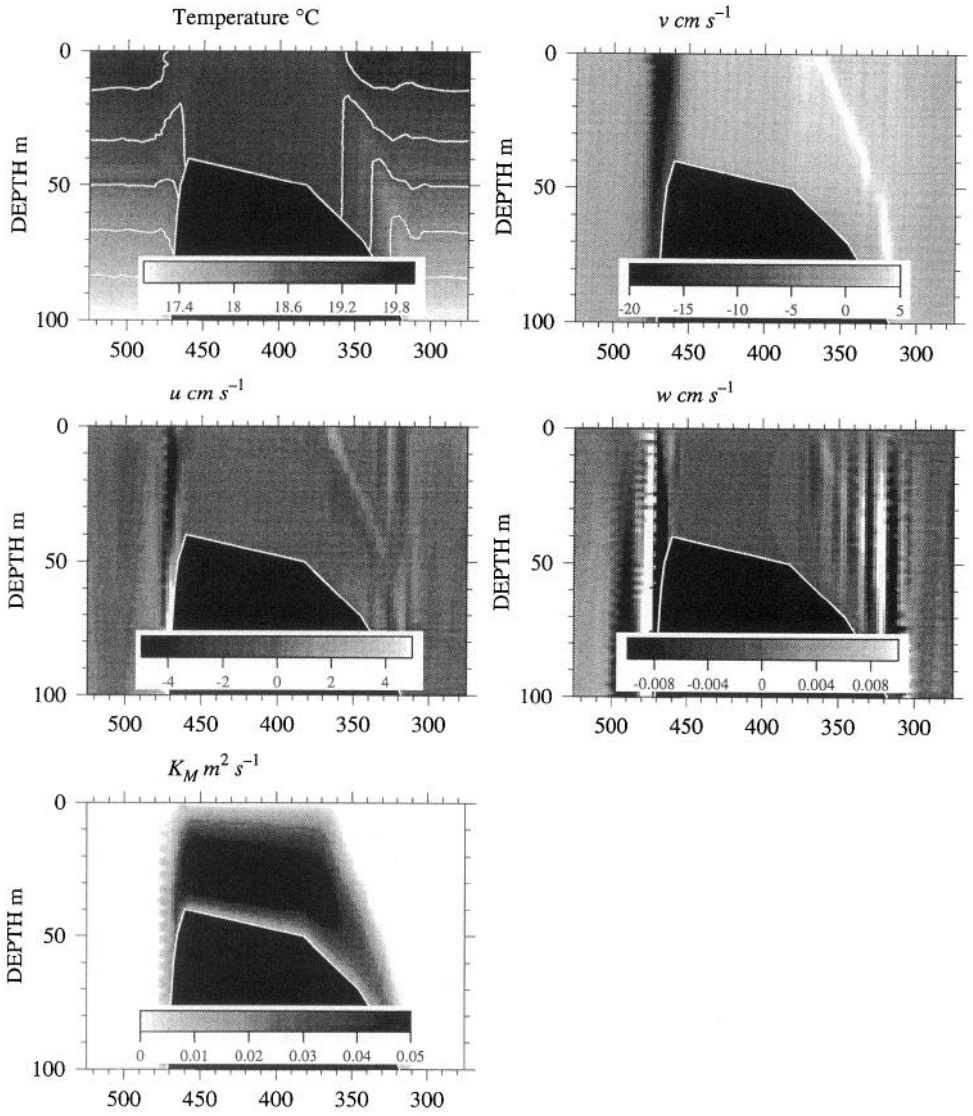

Figure 5. Tidal-average physical fields from tidal cycle 25 of the model. Upper left: temperature, with contours every 0.5°C. Upper right: along-isobath velocity *v*. Dark values are into the page, light values out of the page. Middle left: cross-bank velocity *u*. Dark values are to the right, light values to the left. Middle right: vertical velocity *w*. Dark values are downward, light values are upward. Bottom: vertical eddy diffusivity, K_M.

stratified tidal nonlinear interactions and tidal mixing. The strongest cells were located near the steep portion of the shelf break; weaker cells were found in the shallow, well-mixed waters. Maximal cross-bank velocities reached 5 cm s^{-1}, while maximal upwelling velocities were about 0.1 cm s^{-1}. A strong single-celled circulation developed in the

northern front, with cross-bank velocities reaching 10 cm s^{-1}, and downwelling velocities of 0.3 cm s^{-1}. This cell downwelled water along the sloping bottom to a depth of about 150 m, with upwelling on the northern side of the tidal front. Over the bank, the well-mixed waters showed a residual current flowing to the south, with a speed of about 0.6 cm s^{-1} at the surface, and 0.1 cm s^{-1} at the bottom.

The mean vertical eddy viscosity, K_M, showed maximal values in the shallow, well-mixed waters on the top of the bank (Fig. 5). A subsurface maximum of >0.05 m^2 s^{-1} developed on the bank, while values <0.02 m^2 s^{-1} were found off the bank. While the region of elevated vertical eddy viscosity extended to the same depth on both sides of the bank, the more gentle slope on the southern side gave a broader region of enhanced mixing, associated with the multi-celled circulations in and around the tidal front.

The physical dynamics on and around the bank are very complicated due to the tidal mixing fronts, the generation of internal tides, and the modification of vertical mixing due to stratification. Because of this, the tidal-average fields do not represent the details of flows during a tidal cycle. Some of these details will be explored below in the study of the northern tidal front.

Biological. Tidal-average biological fields from the 25th tidal cycle show striking modifications of the initial conditions (Fig. 6). The phytoplankton field became vertically homogeneous on the top of the bank, with slightly decreasing concentrations from south to north. A subsurface maximum (~4 μmole N l^{-1}) developed at about 18 m depth in the stratified waters off the bank. A patch of high phytoplankton biomass (~5 μmole N l^{-1}) formed in the northern tidal front, stretching from the surface at the front to the depth of the subsurface phytoplankton maximum layer off the bank. Inside the tidal fronts, the phytoplankton concentrations were high down to the bottom, with a tongue of high biomass (~3 μmole N l^{-1}) extending down the northern flank of the bank. These distributions closely resemble those shown in O'Reilly *et al.* (1987) and Horne *et al.* (1989) for phytoplankton on and around Georges Bank during the summer.

The phytoplankton distributions were mirrored by the dissolved nutrient distributions, which showed very low values on the bank, and a sharp nutricline off the bank at about 25–30 m depth. On the flanks of the bank, the nutricline became horizontal, following the tidal fronts. Tongues of higher nutrient concentration (~3 μmole N l^{-1}) could be seen extending toward the surface in the fronts. Inshore of these upward-extending tongues, the low nutrient concentrations extended down the flanks of the bank, reaching ~100 m on the northern flank. Very strong horizontal gradients of dissolved nutrients developed between the waters on top of the bank, and off the bank, particularly below the euphotic zone.

The zooplankton populations like the phytoplankton and dissolved nutrients, were homogenized on the bank, but their concentration increased from south to north, in the opposite sense of the phytoplankton gradient. The highest zooplankton concentrations were found in the unperturbed waters off the bank, separated from the well-mixed waters on the bank by a region of very low zooplankton concentration.

The highest nutrient uptake rates were found at the surface, in the well-mixed waters of

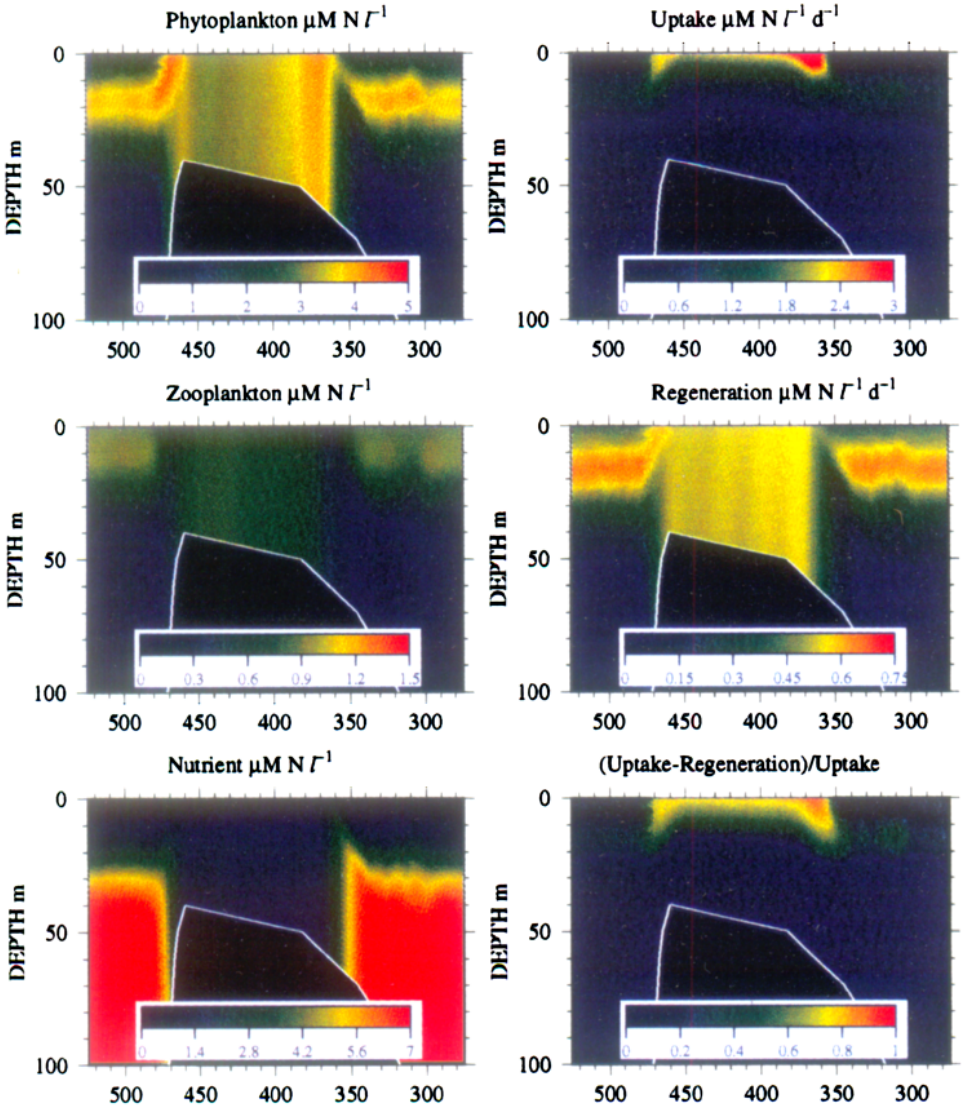

Figure 6. Tidal-average biological fields from tidal cycle 25 of the model. Left panels: top, phytoplankton; middle, zooplankton; bottom, nutrients. Note the different scales. Right panels: top, uptake rate of nutrients by phytoplankton; middle, regeneration rate of nutrients by zooplankton and dead phytoplankton; bottom, surrogate f ratio. Bottom right panel is proportion of phytoplankton uptake *not* accounted for by regeneration, i.e., new production.

the bank, with tongues of high uptake rates extending downward along the two tidal fronts. Maximal uptake rates were about 4.5 μmole N l^{-1} d^{-1}, at the surface in the southern front. Regeneration rates of nutrients were quite low, with maximal rates of 0.75 μmole N l^{-1} d^{-1} in the subsurface phytoplankton maximum layers off the bank. Rates were quite uniform over the bank, strongly decreasing off the bank below the euphotic zone.

The first term on the right-hand side of Eq. (1) is the rate of uptake of nutrients by phytoplankton (units: μmole N l^{-1} s^{-1}). The last three terms on the right-hand side of Eq. (3) are zooplankton excretion, and death of zooplankton and phytoplankton (units: μmole N l^{-1} s^{-1}): the rate of regeneration of nutrients. The *f* ratio (Dugdale and Goering, 1967; Eppley and Peterson, 1979) is the ratio of new:total production, with total production being the sum of new plus recycled production. In this model, the uptake of nutrients is equivalent to total production, and regenerated nutrients fuel recycled production. Assuming recycled nutrients to be taken up in preference to new nutrients (i.e., ammonium is taken up before nitrate; Conway, 1977; Collos, 1989), the *f* ratio can be calculated from the fraction of total production *not* accounted for by recycled production, i.e., (uptake − regeneration)/uptake. This ratio of production supported by non-regenerated nutrients to total production showed values up to 0.7 at the surface of the southern front. Values of 0.5–0.8 were found in the surface waters of the bank and the fronts, with values of 0.1–0.2 off the bank. These values suggest a system on the bank which is strongly supported by the flux of new nutrients, surrounded by regions in which production is maintained largely by recycled nutrients. The high values of the *f* ratio at the surface of the fronts indicate that the phytoplankton patches in these regions are growing largely on nutrients supplied from the aphotic zone by the frontal dynamics.

b. Dynamics in the northern front

Strong asymmetries in cross-bank velocity structure and vertical mixing can be seen on the northern flank during different phases of the tidal cycle (Fig. 7). The flood tide was defined as on-bank flow to the north ($u > 0$; from right-to-left in the figures). During full flood, a strong horizontal gradient in u (cross-front velocity) leads to very strong downwelling of water along the northern flank, and upwelling offshore of the front. At the flood-to-ebb transition, the velocities are weak, but the vertical mixing increases within the front, reaching values of 1 m^2 s^{-1}. The horizontal gradient of u is much weaker during full ebb than full flood, leading to a somewhat weaker cross-frontal circulation cell. The major periods of vertical mixing are confined to full flood just inshore of the front, and the flood-to-ebb transition within the front. The strong asymmetries in patterns and dynamics during opposite phases of the tidal cycle are consistent with observations of Loder *et al.* (1992) in this region.

The time series of phytoplankton concentration over a tidal cycle in the northern front (Fig. 8) shows strong asymmetries in features during a cycle, driven by the advection and mixing. The nutrient patterns are mirror images of the phytoplankton patterns, with low nutrient concentrations in regions of high phytoplankton biomass, and vice versa. As the

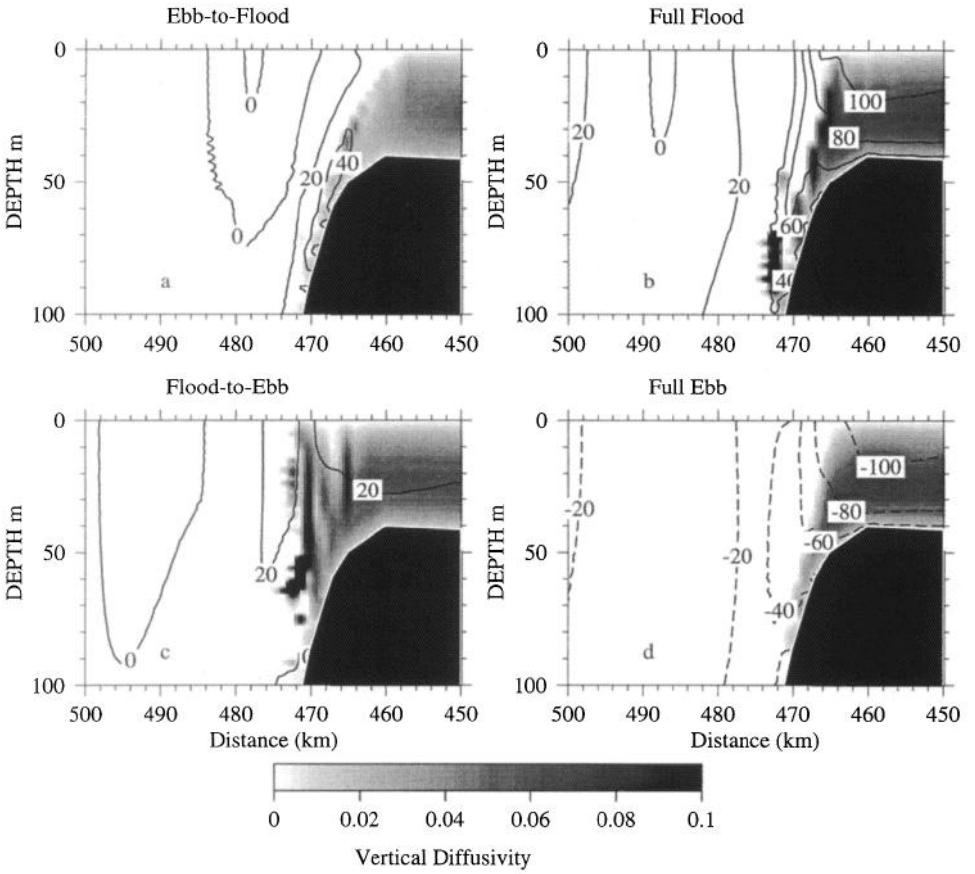

Figure 7. Vertical eddy viscosity K_M (shading) and cross-front velocity u (contours), on the northern flank of the bank during four phases of the tidal cycle. Gray scale gives values of K_M in $m^2\ s^{-1}$; contour of u in $cm\ s^{-1}$. Solid contours ($u > 0$) indicate velocities to the left.

tide floods over the bank, the inshore portion of the phytoplankton patch is advected downward along the flank of the bank. This creates very strong horizontal gradients by the flood-to-ebb tide transition. Exceptionally strong vertical mixing during the flood-to-ebb transition led to a pulse of nutrient-rich water into the euphotic zone, and downward mixing of phytoplankton (also see Fig. 10 below). This asymmetric mixing caused by the tidal propagation over the bank maintained a constant supply of new nutrients to the phytoplankton in the front, allowing the formation of a patch there. During the ebb tide, vertical mixing increased on the bank. This vertical mixing, combined with vertical shearing of the cross-frontal flows, transported nutrients mixed upward during the flood-to-ebb transition horizontally onto the bank where they fueled new production. This transport is consistent with mixing due to a breaking internal tide as described by Brickman and Loder (1993).

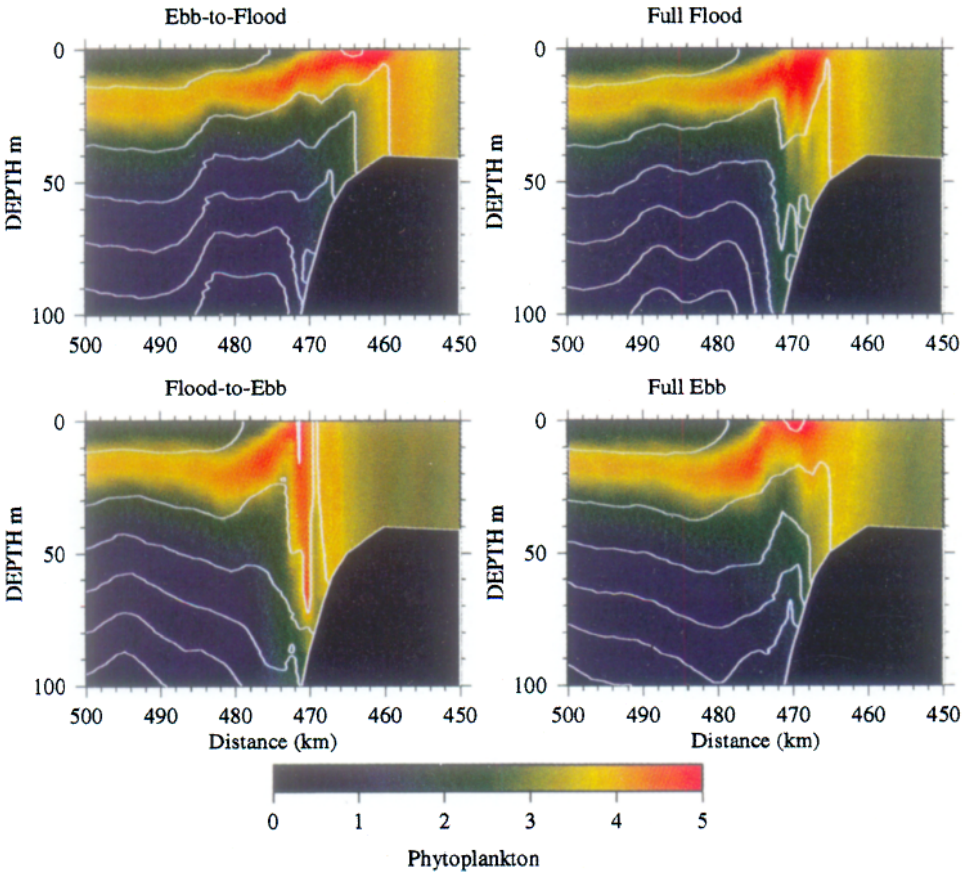

Figure 8. Phytoplankton (colors) and temperature (contours every 0.5°C) during the same four phases of the tide as in Fig. 7. Color scale for phytoplankton in μmole N l^{-1}.

The portion of the tidal cycle during which the bulk of the nutrients are transported vertically into the euphotic zone of the front lasts only about 2 h. The mixing is concentrated over a 10 km region which is very dynamic vertically and horizontally. It is this region, within and just offshore of the maximal horizontal temperature gradient, where the nutrients fueling new production on the bank are brought toward the surface and across the front. It is likely, given the difficulties in sampling from such a region and the transient nature of the flux, that this cross-frontal nutrient transport has not been well sampled in the field for any tidal front. It would be easy to miss the significant portion of the tidal cycle, or the region of maximal nutrient flux with most sampling technologies.

c. Comparison to data

A comprehensive data set for nutrients and phytoplankton on Georges Bank during summer can be found in Horne *et al.* (1989). The distributions of phytoplankton and nitrate

found in that study agree both qualitatively and quantitatively with the distributions developed in the present model. The patterns of phytoplankton and nitrate, for example the homogenized distributions on the bank, the patch of high biomass in the northern front, the strong subsurface horizontal gradients across the fronts, and the tongues of high nutrient extending upward in the fronts are all seen in both the model and data. The concentrations of properties also agree well with the data: phytoplankton concentrations of 3.5–4.5 μmole Nl^{-1} on the bank correspond to about 3–5 μg chl *a* l^{-1} seen in the well mixed waters of the bank (O'Reilly *et al.,* 1987; Horne *et al.,* 1989; their Fig. 2g). The strong cross-frontal nutrient gradients at depth are also quantitatively reproduced by the model.

For comparison to the data of Horne *et al.* (1989; their Table 1), the model data were averaged over the euphotic zone ($-\ln(0.01)/k_{ext} \sim 46$ m) (Fig. 9). The data from Horne *et al.* were multiplied by their euphotic depths to give euphotic zone averages. Their dissolved nitrate and ammonium concentrations were added for comparison to our model data, as were the nitrate and ammonium uptake rates. The data from Horne *et al.* are plotted in the appropriate regions, and show excellent agreement with the model. In particular, the model uptake rates show striking agreement with those measured on the bank. Although no ammonium regeneration rates were measured by Horne *et al.,* these data have been presented in Figure 9 for comparison to the uptake rates.

Horne *et al.* found *f* ratios ranging from 0.04–0.36 in the euphotic zone off the bank, to 0.23–0.70 in the frontal waters, and 0.23–0.31 in the well-mixed waters of the central bank. These values agree very well with the modeled values shown in Figure 6, where the highest proportion of total production supported by non-regenerated nutrients was found in the frontal regions. This pattern is also supported by Sathyendranath *et al.* (1991), who used compound remote sensing to estimate *f* ratios on the bank.

The zooplankton biomass on the bank, $\sim 0.7 - 1$ μmole N l^{-1}, corresponds to a carbon biomass of 25–80 μg C l^{-1}, depending on the choice of C:N ratio. This includes the range of 30–50 μg C l^{-1} presented in Davis (1987) for copepod biomass on the central bank during summer. The distributions of zooplankton—well mixed with moderate abundances on the bank, higher abundances at the surface off the bank—corresponds to those found by Perry *et al.* (1993) across the northern front of Georges Bank.

The nutrient uptake rates can be integrated vertically in the well-mixed region of the bank for comparison to Hopkins and Garfield's (1981) estimate of 2 g C m^{-2} d^{-1} for the primary production of the central bank. We defined the well-mixed region to be the waters in which the modeled vertical temperature gradient was <0.5°C (our estimates were almost the same using 0.1°C). Integrating vertically and horizontally in these waters, we obtained a mean uptake rate of 37.9 mmol N m^{-2} d^{-1}, or about 3 g C m^{-2} d^{-1} using the Redfield C:N ratio for phytoplankton. Had we taken only the most central bank uptake values, our estimate would have been much lower. This is because a significant amount of primary production takes place just inside the tidal fronts, where the nutrients are plentiful yet the waters are still well mixed. Thus we feel that our estimates may actually be more accurate than those obtained from only a few stations. Still, the agreement is good between the modeled and measured primary production estimates.

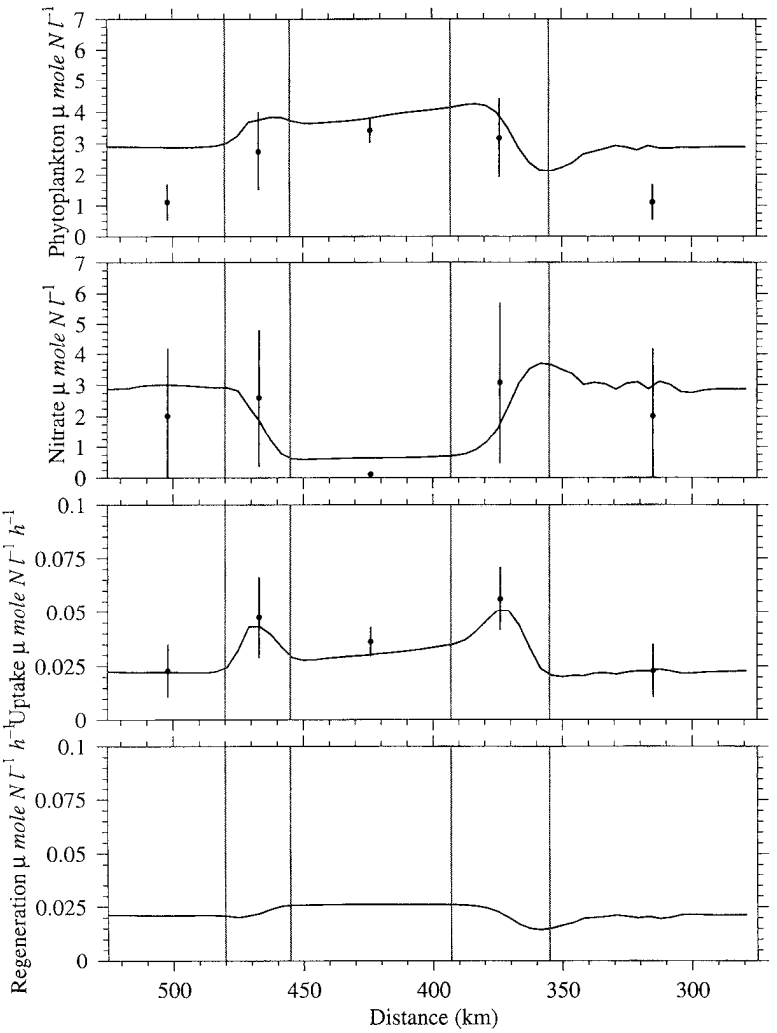

Figure 9. Euphotic zone averages of phytoplankton (top), nutrient (2nd from top), phytoplankton nutrient uptake rate (2nd from bottom) and nutrient regeneration rate (bottom). Vertical lines divide the various regions of the bank. From left to right: stratified, northern front, central, southern front, stratified. Data points and standard deviations are calculated from data in Horne *et al.* (1989) Table 1.

d. Fluxes and new production

To calculate the physically forced fluxes of properties on and off the bank, we ran the model for 25 tidal cycles with all the biological dynamics included, and then turned off all the biological interactions for two tidal cycles. Thus the biological variables behaved as conservative, independent passive tracers during the last two tidal cycles. Taking the difference between the two biologically inactive cycles, we could quantify the physically forced fluxes of phytoplankton, zooplankton and nutrients on and off the bank (Fig. 10).

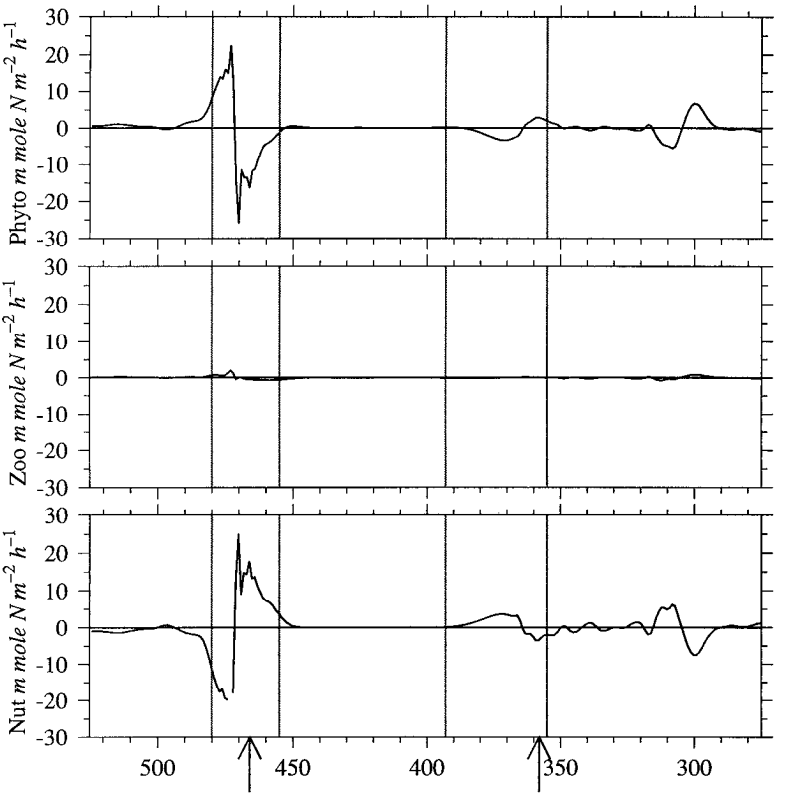

Figure 10. Physically forced vertically integrated fluxes of phytoplankton (top), zooplankton (middle) and nutrient (bottom) over a tidal cycle. No biological interactions occurred during this tidal cycle; biological variables behaved as conservative, passive tracers. Positive values indicate an increase in that region. Arrows indicate the region of the bank where the model top-to-bottom temperature difference was <0.5°C.

The nutrient and phytoplankton fields mirrored each other almost exactly, indicating a strong coupling between the two fields. The fluxes of zooplankton were a factor of 10 lower than the phytoplankton or nutrient fluxes due to lower biomasses. Increases of nutrients were seen on the bank, and inshore of the tidal fronts, with balancing decreases on the off-bank sides of the fronts. The largest changes occurred within the fronts, where nutrients were transported from deep waters toward the shallow waters of the bank.

The rates of physical nutrient transfer can be compared to nutrient uptake and regeneration rates to get an alternate estimate of the *f* ratio. Taking our earlier estimate of 37.9 mmol N m^{-2} d^{-1} for the total production in the well-mixed waters of the bank, we can perform the same integration to calculate the rate of nutrient regeneration in the same waters: 26.7 mmol N m^{-2} d^{-1}. Assuming that regenerated nutrients are taken up in preference to physically transported nutrients, an *f* ratio calculated from these values is about 0.3 (1–26.7/37.9). This value falls within the range measured by Horne *et al.* (1989)

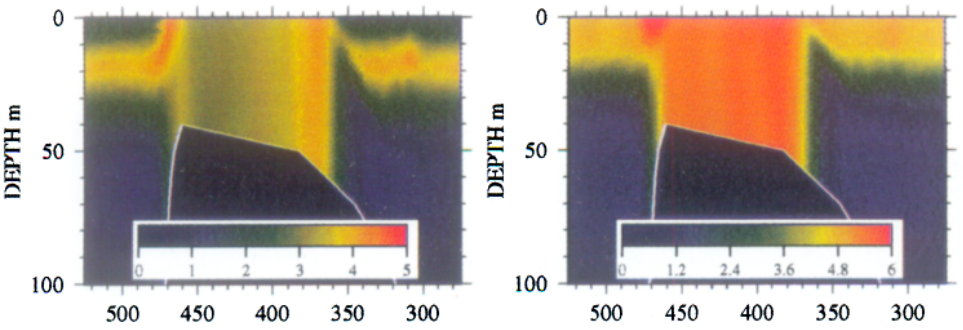

Figure 11. Comparison of sinking (left) and non-sinking (right) cases for phytoplankton. Note the different scales for the biomass.

for the central bank waters (0.23–0.31), and suggests that only a third of the total production in the well-mixed waters is supported by new nutrients.

The rate of nutrient transport to the well-mixed waters of the model bank was calculated to be 23.3 mmol N m^{-2} d^{-1}. In principal, these new nutrients could support production with an *f* ratio of 23.3/37.9 = 0.61. The relatively high rate of supply of regenerated nutrients, however, suggests that the phytoplankton in the well-mixed waters of Georges Bank are nutrient replete, with an excess of nutrients supplied by physical processes. This same conclusion was reached by Schlitz and Cohen (1984) and Horne *et al.* (1989), who calculated rough nutrient budgets for the bank.

One important observation from the model is that these values for production in the well-mixed waters of Georges Bank may be significant underestimates of the total bank production: a significant fraction of the primary production occurs in the tidal fronts. This production is spatially restricted in a very dynamic environment, and supported largely by nutrients supplied by physical transports from below the euphotic zone off the bank (Fig. 10). The temporal transience of the biological features in the fronts, particularly the northern front, and the small spatial scale of the patches would make field estimation of this frontal production very difficult. Cross-frontal nutrient transports appear to be driven by a nonlinear coupling of advection and diffusion, with the largest transports occurring during only a few hours of the tidal cycle.

There have been several suggestions that sinking or swimming in cross-frontal flows may be responsible for plankton patchiness at fronts (e.g., Franks, 1992a; Pingree *et al.*, 1975; Savidge, 1976). In the present model, the inclusion of a constant sinking velocity led to the creation of a subsurface phytoplankton maximum off the bank, but had very little influence on the formation of the patches of phytoplankton in the fronts (Fig. 11). With no sinking at all, a patch of slightly higher biomass formed at the northern tidal front. This was due to the fact that there was no sinking loss of cells from the euphotic zone. The patch was less elongate in the offshore direction than in the sinking case. It is apparent, however, that sinking or swimming is not a prerequisite for patch formation at tidal fronts. Rather, the

strong physical dynamics, forcing nutrient fluxes to the frontal euphotic zone, is the primary factor regulating phytoplankton patch formation.

The strong physical forcing on the bank also causes local decoupling of trophic interactions: vertical mixing decreases the average zooplankton concentration, allowing growth of the phytoplankton on the bank and in the patches at the fronts. This reduction in grazing pressure, coupled with nutrient pumping from the aphotic zone, stimulates phytoplankton growth leading to the formation of patches and high rates of new production. The qualitative and quantitative agreement of the modeled biological patterns and fluxes with the field data from Georges Bank suggest that patterns of biomass and fluxes of the summertime planktonic ecosystem on the bank result from physically forced decoupling of trophic dynamics. The similar patterns of phytoplankton and nutrients at other tidal fronts (e.g., Holligan, 1981; Pingree *et al.,* 1975; reviews in LeFevre, 1986; Franks, 1992b) suggests that these dynamics are not restricted to just the Georges Bank fronts, but may be more widely applicable.

The qualitative aspects of the model's results are quite robust, i.e., the location of the horizontal gradients, the well-mixed waters on the top of the bank, and the formation of a phytoplankton patch in the northern front do not change under a wide range of parameters. We tested the model with a range of the diffuse attenuation coefficient k_{ext}, the half-saturation constant for nutrient uptake k_s, the total amount of nutrient N_T, the sinking speed w_s, and the grazing parameters R_m and λ. While biomasses changed, and the depth of the nutricline varied with changes in k_{ext}, the basic patterns of biological variables remained the same. The inclusion of a spatially variable flux of nutrients from the bottom had almost no effect on the results, as the fluxes (1–10 μmole m^{-2} h^{-1}, e.g., Walsh *et al.,* 1987) were much lower than the regenerated or physically forced fluxes on the bank. This same conclusion was reached by Thomas *et al.* (1978), who studied regeneration and primary production on the bank. These results give us confidence that the dynamics we have simulated are robust, and may accurately reflect the dynamics controlling plankton distributions on Georges Bank.

5. Conclusions

The strong physical forcing by the M_2 tide over Georges Bank perturbed the steady-state distributions of phytoplankton, zooplankton and nutrient to a close approximation of the fields measured on the bank during the summer. Estimates of phytoplankton nutrient uptake rates and supply rates of new nutrients to the bank agreed well with available data. New production was reasonably high in the well-mixed portion of the bank, where f ratios were ~0.3. The high values of f in the fronts (up to 0.7) reflected the pumping of new nutrients up from below the euphotic zone. This pumping was very spatially and temporally restricted, occurring largely during a 2 h period of the tidal cycle. The steep topography of the northern flank led to enhanced new production in the northern front, and the formation of a phytoplankton patch within the front. This frontal region represents a high proportion of the total and new production on the bank. The strong variability of this

feature over a tidal cycle suggests that accurate sampling of such a patch would be extremely difficult.

Acknowledgments. PJSF would like to thank Dr. Brian Osborne for donating his copy of "Georges Bank," which greatly facilitated this study. The encouragement of Drs. Glen Gawarkiewicz, Tom Powell and William Peterson is gratefully acknowledged. This paper is funded in part by grant NA36GP0320 to PJSF, and WHOI subcontracts RR50662F and RR50662FCI to CC, from the National Oceanic and Atmospheric Administration. The views expressed herein are those of the authors and do not necessarily reflect the views of NOAA or any of its sub-agencies. This is contribution 67 of the U.S. GLOBEC program, funded jointly by NOAA and NSF.

REFERENCES

Bienfang, P. K. 1981. SETCOL—a technologically simple and reliable method for measuring phytoplankton sinking rates. Can. J. Fish. Aquat. Sci., *38,* 1289–1294.

Blumberg, A. F. 1994. A primer of ECOM3D-si. Technical Report, HydroQual, Inc. Mahwah, NJ, 84 pp.

Blumberg, A. F. and G. L. Mellor. 1987. A description of a three-dimensional coastal ocean circulation model, *in* Three-Dimensional Coastal Ocean Models, N. S. Heaps, ed., Coast. and Estuarine Sci., *4,* 1–16.

Brickman, D. and J. W. Loder. 1993. Energetics of the internal tide on northern Georges Bank. J. Phys. Oceanogr., *23,* 409–424.

Casulli, V. 1990. Semi-implicit finite-difference methods for the two-dimensional shallow water equations. J. Comp. Phys., *86,* 56–74.

Chen, C. and R. C. Beardsley. 1995. A numerical study of stratified tidal rectification over a finite-amplitude symmetric banks. J. Phys. Oceanogr., *25,* 2090–2110.

Chen, C., R. C. Beardsley and R. Limeburner. 1995. A numerical study of stratified tidal rectification over Georges Bank. J. Phys. Oceanogr., *25,* 2111–2128.

Cohen, E. B. and M. D. Grosslein. 1987. Production on Georges Bank compared with other shelf ecosystems, *in* Georges Bank, R. H. Backus, ed., The MIT Press, Cambridge, MA, 383–391.

Cohen, E. B., M. D. Grosslein, M. P. Sissenwine, F. Steimle and W. R. Wright. 1982. Energy budget of Georges Bank. Can. Spec. Pub. Fish. Aquat. Sci., *59,* 95–107.

Collos, Y. 1989. A linear model of external interactions during uptake of different forms of inorganic nitrogen by microalgae. J. Plankton Res., *11,* 521–533.

Conway, H. L. 1977. Interactions of inorganic nitrogen in the uptake and assimilation by marine phytoplankton. Mar. Biol., *39,* 221–232.

Davis, C. S. 1987. Zooplankton life cycles, *in* Georges Bank, R. H. Backus, ed., The MIT Press, Cambridge, MA, 256–267.

Dugdale, R. C. and J. J. Goering. 1967. Uptake of new and regenerated forms of nitrogen in primary productivity. Limnol. Oceanogr., *12,* 196–206.

Eppley, R. W. and B. J. Peterson. 1979. Particulate organic matter flux and planktonic new production in the deep ocean. Nature, *282,* 677–680.

Eppley, R. W., J. N. Rogers and J. J. McCarthy. 1969. Half-saturation constants for uptake of nitrate and ammonium by marine phytoplankton. Limnol. Oceanogr., *14,* 912–920.

Falkowski, P. G. 1975. Nitrate uptake in marine phytoplankton: comparison of half-saturation constants from seven species. Limnol. Oceanogr., *20,* 412–417.

Flagg, C. N. 1987. Hydrographic structure and variability, *in* Georges Bank, R. H. Backus, ed., The MIT Press, Cambridge, MA, 108–124.

Franks, P. J. S. 1992a. Sink or swim: accumulation of biomass at fronts. Mar. Ecol. Prog. Ser. *82,* 1–12.

—— 1992b. Phytoplankton blooms at fronts: patterns, scales, and physical forcing mechanisms. Rev. Aquat. Sci., *6,* 121–137.

Franks, P. J. S., J. S. Wroblewski and G. R. Flierl. 1986. Behavior of a simple plankton model with food-level acclimation by herbivores. Mar. Biol., *91,* 121–129.

Fransz, H. G., J. M. Colebrook, J. C. Gamble and M. Krause. 1991. The zooplankton of the North Sea. Netherlands J. Sea Res., *28,* 1–52.

Garrett, C. J. R. and J. W. Loder. 1981. Dynamical aspects of shallow sea fronts. Phil. Trans. R. Soc. Lond., *A302,* 563–581.

Granata, T. C. 1991. Diel periodicity in growth and sinking rates of the centric diatom *Coscinodiscus concinnus.* Limnol. Oceanogr., *36,* 132–139.

Holligan, P. M. 1981. Biological implications of fronts on the northwest European continental shelf. Phil. Trans. R. Soc. Lond., *A302,* 547–562.

Hopkins, T. S. and N. Garfield III. 1981. Physical origins of Georges Bank water. J. Mar. Res., *39,* 465–500.

Horne, E. P. W., J. W. Loder, W. G. Harrison, R. Mohn, M. R. Lewis, B. Irwin and T. Platt. 1989. Nitrate supply and demand at the Georges Bank tidal front. Scient. Mar., *53,* 145–158.

Le Fevre, J. 1986. Aspects of the biology of frontal systems. Adv. Mar. Biol., *23,* 163–299.

Loder, J. W., D. Brickman and E. P. W. Horne. 1992. Detailed structure of currents and hydrography on the northern side of Georges Bank. J. Geophys. Res., *97,* 14331–14351.

Loder, J. W. and T. Platt. 1985. Physical controls on phytoplankton production at tidal fronts, *in* Proceed. of the 19th Europ. Mar. Biol. Symp., P. E. Gibbs, ed., Cambridge Univ. Press, Cambridge, UK, 3–22.

Loder, J. W., D. G. Wright, C. Garrett and B.-A. Juszko. 1982. Horizontal exchange on central Georges Bank. Can. J. Fish. Aquat. Sci., *39,* 1130–1137.

Mellor, G. L. and T. Yamada. 1982. Development of a turbulence closure model for geophysical fluid problems. Rev. Geophys. Space Phys., *20,* 851–875.

Moody, J. A., B. Butman, R. C. Beardsley, W. S. Brown, P. Daifuku, J. D. Irish, D. A. Mayer, H. O. Mofjeld, B. Petrie, S. Ramp, P. Smith and W. R. Wright. 1984. Atlas of tidal elevation and current observations on the northeast American continental shelf and slope. U.S. Geological Survey Bull., 1611.

O'Reilly, J. E., C. Evans-Zetlin and D. A. Busch. 1987. Primary production, *in* Georges Bank, R. H. Backus, ed., The MIT Press, Cambridge, MA, 220–233.

Pastuszak, M., W. R. Wright and D. Patanjo. 1982. One year of nutrient distribution in the Georges Bank region in relation to hydrography, 1975–1976. J. Mar. Res., *40* (Supp), 525–542.

Perry, R. I., G. C. Harding, J. W. Loder, M. J. Tremblay, M. M. Sinclair and K. F. Drinkwater. 1993. Zooplankton distributions at the Georges Bank frontal system: retention or dispersal? Cont. Shelf Res., *13,* 357–383.

Pingree, R., P. Pugh, P. Holligan and G. Forster. 1975. Summer phytoplankton blooms and red tides in the approaches to the English Channel. Nature, *258,* 672–677.

Riley, G. A. 1941. Plankton studies. IV. Georges Bank. Bull. Bingham Oceanogr. Coll. *7,* 1–73.

Sathyendranath, S., T. Platt, E. P. W. Horne, W. G. Harrison, O. Ulloa, R. Outerbridge and N. Hoepffner. 1991. Estimation of new production in the ocean by compound remote sensing. Nature, *353,* 129–133.

Savidge, G. 1976. A preliminary study of the distribution of chlorophyll *a* in the vicinity of fronts in the Celtic and Western Irish Seas. Estuar. Coastal Mar. Sci., *4,* 617–625.

Schlitz, R. J. and E. B. Cohen. 1984. A nitrogen budget for the Gulf of Maine and Georges Bank. Bio. Oceanogr., *3,* 203–222.

Thomas, J. P., J. E. O'Reilly and C. N. Robertson. 1978. Primary production and respiration over Georges Bank during March and July 1977. I.C.E.S. Biol. Oceanogr. Comm. Doc. CM 1979/L:37, 17 p.

Uchupi, E. and J. A. Austin. 1987. Morphology, *in* Georges Bank, R. H. Backus, ed., The MIT Press, Cambridge, MA, 25–29.

Walsh, J. J., T. E. Whitledge, J. E. O'Reilly, W. C. Phoel and A. F. Draxler. 1987. Nitrogen cycling on Georges Bank and the New York Shelf: a comparison between well-mixed and seasonally stratified waters, *in* Georges Bank, R. H. Backus, ed., The MIT Press, Cambridge, MA, 234–246.

Received: *28 November, 1995;* revised: *11 April, 1996.*